In Vitro and Molecular Docking Studies of the Antimalarial Activities of *Strychnos ligustrina* Extracts from Different Parts of the Woody Stem

Rita Kartika SARI[1,2,3,†] · Wasrin SYAFII[1] · Yanico Hadi PRAYOGO[1] · Anne CAROLINA[1] ·
Sri FAMILASARI[1] · Umi CAHYANINGSIH[4] · Siti SA'DIAH[2,5] · Setyanto Tri WAHYUDI[2,6] ·
Muhammad Adly Rahandi LUBIS[7]

ABSTRACT

Previous studies have shown that the aqueous extract of *Strychnos ligustrina* wood exerts antimalarial activity by inhibiting the growth of *Plasmodium falciparum* strain 3D7. This study determined the extract yields of three different parts of the woody stem of *S. ligustrina* (heartwood, sapwood, and bark), analyzed their phytochemical profiles using liquid chromatography–tandem mass spectrometry (LC-MS/MS), investigated their antimalarial activity against *P. falciparum*, and predicted the active compounds using molecular docking studies. The powdered heartwood, sapwood, and bark were macerated in water (1:10 w/v) for three 24-hour cycles. The heartwood extract had the highest yield (6.62%), followed by bark extract (5.42%) and sapwood extract (4.28%). LC-MS/MS confirmed that all of the extracts contained alkaloids. Strychnine were the dominant components in the heartwood and sapwood extracts. Conversely, the bark extract was dominated by brucine and N-[1-(6,7-dimethoxy-1,2,3,4-tetrahydroisoquinoline-1-ylidene)-4-methyl-2-oxopentan-3-yl]benzamide, whereas it contained minimal strychnine content. The *in vitro* antimalarial assay test showed that the heartwood extract exhibited the highest antimalarial activity (IC_{50} = 10.14 µg/mL), followed by the bark (IC_{50} = 16.46 µg/mL), and sapwood extracts (IC_{50} = 17.30 µg/mL), with all extracts categorized as strong antimalarial compounds (IC_{50} < 20 µg/mL). Molecular docking studies predicted that each extract has a specific mechanism against five target proteins with binding affinity values that surpassing those of chloroquine (positive control).

Keywords: bark, heartwood, liquid chromatography–tandem mass spectrometry, *Plasmodium falciparum* strain 3D7, sapwood

1.　INTRODUCTION

Malaria is a tropical infectious disease with a high mortality rate, caused by *Plasmodium* species. There were 249 million malaria cases worldwide in 2022, 5 million more than in 2021, significantly exceeding pre-COVID-19 number (World Health Organization, 2023). In the WHO's Southeast Asia Region, almost 94% of all malaria-related deaths occurred in Indonesia (World Health Organization, 2023). According to the Indonesian Ministry of Health (2023), the number of malaria cases increased significantly to 3.3 million in 2022, a 64.6% increase compared to 2021. One of the obstacles to providing effective malaria therapy is that *Plasmodium* parasites can acquire resistance to antimalarial drugs. The preferred antimalarial drugs have changed several times, starting with chloroquine before shifting to sulfa-doxine/pyrimethamine and artemisinin (Giacometti *et al.*, 2021). The risk of emerging resistance can be minimized by using artemisinin-based combination therapy along-side primaquine or natural antimalarial bioactive subs-tances (Huynh, 2016).

The *Strychnos* genus has been traditionally used to treat malaria in Asia and Africa. *Strychnos* species produce antimalarial substances (Philippe *et al.*, 2005). *Strychnos ligustrina* Blume syn. *Strychnos lucida* R. (Indonesia: Kayu ular/Bidara laut/Songga), a plant that grows abundantly in Indonesia, has been traditionally used as an antimalarial remedy. Indonesian traditional medicine has long utilized Strychnos plants to formulate treatments for malaria (Setiawan *et al.*, 2014; Taek, 2023). Several studies have demonstrated the *in vitro* antimalarial activity of aqueous extracts of *S. ligustrina* wood (Familasari *et al.*, 2023; Manurung *et al.*, 2019), and these findings were confirmed *in vivo* (Cahyaningsih *et al.*, 2022, 2023). The effective doses identified via *in vivo* antimalarial assays are safe for consumption, as demonstrated by subchronic toxicity (Sadiah *et al.*, 2023) and acute oral toxicity tests (Khasanah *et al.*, 2024).

Consequently, there is potential to develop medications using the aqueous extract of *S. ligustrina* wood as a cost-effective active ingredient in antimalarial drugs.

Despite extensive research on the bioactive com-pounds and pharmacological potential of *S. ligustrina*, the antimalarial potential of different woody stem parts (heartwood, sapwood, and bark) has not been thoroughly investigated. Previous studies of *S. ligustrina* extract as an antimalarial did not separate the sapwood and heart-wood parts, and did not use bark (Manurung *et al.*, 2019; Syafii *et al.*, 2016). Heartwood is the stem's center and is usually darker than the outer sapwood. Sapwood is the outer part of the wood, and its cell tissue remains alive, transporting water and nutrients from the roots to the leaves. The bark is the outermost layer of the tree, serving as a protective barrier. Previous studies have revealed that various wood parts influence the phytochemical composition and biological activity of extracts (Aulia *et al.*, 2022; Ella Nkogo *et al.*, 2022; Miranda *et al.*, 2017; Prayogo *et al.*, 2023; Zalsabila *et al.*, 2024). However, the compounds that can be used as standard antimalarial compounds for *S. ligustrina* wood have not yet been determined.

Molecular docking studies on compounds identified by liquid chromatography–tandem mass spectrometry (LC-MS/MS) can be performed to determine the profile of active compounds in *S. ligustrina* wood with potential antimalarial activity. These advanced analytical techni-ques enable the precise identification and quantification of bioactive constituents, providing valuable insights into their therapeutic potential and mechanisms of action. This research is critical in drug development, as it offers a cost-effective and efficient approach to screening natural products for antimalarial activity (Orozco *et al.*, 2024). Therefore, this study aimed to determine the yields of heartwood, sapwood, and bark extracts of *S. ligustrina*, examine their *in vitro* antimalarial activity, and analyze the active compound profiles of these extracts using LC-MS/MS and *in silico* studies. This research is expec-

ted to contribute to the growing body of evidence supporting the use of plant-derived compounds against malaria, potentially leading to the discovery of new, affordable, and effective treatments.

2. MATERIALS and METHODS

2.1. Plant material collection

S. ligustrina trees were obtained in Dompu, West Nusa Tenggara, Indonesia. This tree herbarium was identified by the Silviculture Laboratory of the Forestry Department, Mataram University, Mataram, Indonesia (voucher 23-2-2023). Woody stems (logs) were taken from three trees with 15−17-cm diameters. These stems were divided into bark, heartwood, and sapwood. The segments were processed into a fine powder (40−60 mesh) using a Willey mill. A test sample weighing ± 2 g was dried in an oven at $103 ± 2℃$ until a consistent dry weight was attained to determine the powder's moisture content (Arinana *et al.,* 2024).

2.2. Extraction of *Strychnos ligustrina*

The powdered heartwood, sapwood, and bark were subjected to maceration using water at a 1:10 (w/v) ratio of powder to solvent. The extraction was performed over three 24-h cycles. The resultant filtrates were combined using a vacuum evaporator at 50℃ to obtain a dry extract. The extraction yield was then calculated.

2.3. Phytochemical compound analysis using liquid chromatography−tandem mass spectrometry

Phytochemical compound analysis was conducted using an ultra-high-performance liquid chromatography system (Vanquish UHPLC) coupled with a Tandem Q Exactive Plus Orbitrap HRMS (Q Extractive Orbitrap MS/MS, Thermo Fisher Scientific, Waltham, MA, USA)

and an Accucore™ C18 column with dimensions of 100 × 2.1 mm and a particle size of 1.5 μm (Catalogue number: 27101-102130, Thermo Fisher Scientific). Each of the three types of extracts was dissolved using methanol LCMS Grade (Merck, Darmstadt, Germany), then filtered with PTFE membrane syringe filter type SYTF (mdi Membrane Technologies, Camp Hill, PA, USA). Gradient elution was performed over 50 minutes at a flow rate of 0.2 mL/min to separate the phytochemical compounds. H_2O with 0.1% formic acid (A) and Acetonitrile with 0.1% formic acid (B) were used as mobile phases in the gradient elution system, with the following steps: 0−1 min (95% A and 5% B), 1−25 min (95%−5% A and 5%−95% B), 25−28 min (95% A and 5% B), and 28−30 min (95% A and 5% B). Positive electrospray ionization was employed as the ionization technique, and Q-Orbitrap was used as the mass analyzer. In both MS and MS/MS modes, the system was set to a range of 100−1,500 m/z with a resolution of 70,000 FWHM, a capillary temperature of 320℃, a column temperature of 30℃, and a spray voltage of (+) 3.8 kV. Additionally, an envelope gas flow rate of 15 mL/min and an auxiliary gas flow rate of 3 mL/min were used. Compound names were identified using the PubChem, COCONUT, and ChemSpider databases. The relative abundance of each compound was calculated by comparing its area percentage to the total area percentage of all compounds (Andianto *et al.*, 2024).

2.4. Antimalarial activity assay

The *in vitro* antimalarial activity assay followed the protocol of Manurung *et al.* (2019) and used the *Plasmodium falciparum* strain 3D7, which is sensitive to chloroquine. The extracts were prepared by dissolving 10 mg of the sample in 1 mL of dimethyl sulfoxide to create a stock solution. Then, serial dilutions were made from the stock solution to obtain concentrations of 1,000 μg/mL, 100 μg/mL, 10 μg/mL, 1 μg/mL, and 0.1 μg/mL.

The parasites used in this test were synchronous (ring stage) with approximately 1% parasitemia (5% hematocrit). Two microliters of the test solution at various concentrations were taken and placed into each well of a 96-well plate. The, 198 μL of the parasite were added (each concentration was made in duplicate). The test well was then inserted into the chamber and exposed to a mixture of gases (5% O_2, 5% CO_2, and 90% N_2). The chamber containing the test wells was incubated for 48 h at 37℃. The cultures were harvested, and thin blood films were made with 20% Giemsa stain.

Under a microscope, the number of infected erythrocytes per 1,000 normal erythrocytes was counted after data analysis on the generated blood smear. After that, the percent growth and inhibition were calculated using the data. The following equations were used to determine percent growth and inhibition, respectively:

$$\% \text{ Parasitemia} = \frac{\Sigma \text{Infected erythrocytes}}{5,000 \text{ Erythrocytes}} \times 100 \quad (1)$$

$$\% \text{ Inhibition} = \frac{\text{Parasitemia test}}{\text{Parasitemia control}} \times 100 \quad (2)$$

To determine the IC_{50} (the concentration of the test material that inhibited the parasite's growth by 50%), statistical analysis was performed using probit analysis based on the percent inhibition data. This analysis involved determining the relationship between the percent inhibition of the parasite and the extract concentrations.

2.5. Molecular docking analysis

The compounds of each extract identified based on LCMS were studied for their molecular binding mechanism to 5 target proteins (Table 1) in the treatment of malaria with the aim of killing the parasite. The selection of protein was limited to proteins that must come

from *P. falciparum* 3D7, according to the one used at the *in vitro* stage. The crystal structure of proteins was obtained from the protein data bank (https://rcsb.org). Ligand preparation was accomplished by limiting the energy of the MM2 approach on the ligand's molecular structure (Chem3D Pro 12.0, CambridgeSoft, Cambridge, MA, USA). AutoDockTools 1.5.6 (The Scripps Research Institute, San Diego, CA, USA) was used to prepare receptors by eliminating non-protein molecules, adding Kolman charges, and adding polar hydrogen. Docking method validation (Redocking) was performed by using the co-crystal ligands in each protein (less than 2 Å). Receptor–ligand binding was visualized using the Discovery Studio Visualizer v.21.1.0.20298 (Dassault Systemes, Vélizy-Villacoublay, France).

3. RESULT and DISCUSSION

3.1. Extract yield and phytochemical profile

The extract yield significantly differed for different woody stem parts of *S. ligustrina* ($p < 0.05$). The heartwood exhibited the highest extract yield, followed by the bark and sapwood (Fig. 1). A higher yield value of heartwood than sapwood was also reported in previous research using *Quercus faginea* (Miranda *et al.*, 2017). The difference in yield is attributable to the different types and phytochemical compositions (Morais and Pereira, 2012). Therefore, if the heartwood and sapwood are not separated, then the extract yield will be diminished, particularly for woody stems with greater sapwood content. The considerable differences in extract yields among heartwood, sapwood, and bark provide valuable insights for optimizing extraction processes and maximizing the efficiency of wood resource utilization.

With the same extraction method, the yield of the aqueous extract of *S. ligustrina* wood in this study (4.28%–6.62%) was higher than that reported by

**Table 1.** List of antimalaria protein target, docking center coordinate, root mean square deviation (RMSD), and role of protein in *Plasmodium falciparum*

Protein (PDB ID)	Center coordinate			RMSD (Å)	Role in antimalaria activity	References
	X	Y	Z			
Lactate dehydrogenase (1ldg)	25.329	23.422	41.843	1.2875	Relating to the anaerobic nature of parasite life	Dunn *et al*. (1996)
M1 Alanylaminopeptidase (3ebh)	14.248	11.055	12.141	1.4307	Involved in the terminal stages of hemoglobin digestion and essential for the provision of amino acids used for parasite growth and development within the erythrocyte.	McGowan *et al*. (2009)
Plasmepsin II (5yib)	18.733	−25.663	−24.032	1.9086	Inhibition plasmepsin protein correlated with hemoglobin catabolism in which parasite survival was depended on host haemoglobin consumption	Mishra et al. (2018)
P*f*NDH2 (5jwc)	29.304	10.210	25.414	1.4617	Inhibition of P*f*NDH2 will inhibit the reaction of ubiquinol formation, which will interfere with the parasite's respiratory system	Yang *et al*. (2017)
Falcylisin (8ho4)	−32.065	5.463	−11.464	0.7339	Inhibition of falcylisin disrupt the short polypeptide cleavage process, resulted accumulation of short poplypeptide in organel	Lin *et al*. (2024); Wirjanata *et al*. (2024)
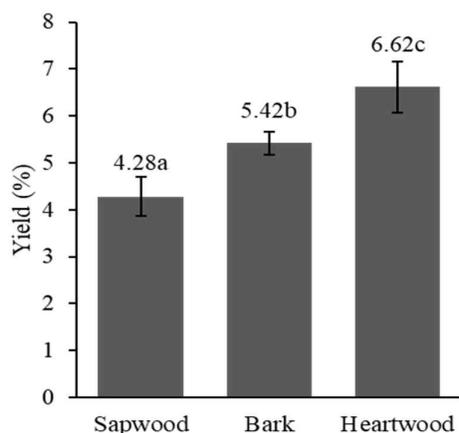
Fig. 1. The yield of *Strychnos ligustrina* extracts for different parts of stem. [a-c] Different letters denote significant differences ($p < 0.05$) as determined using Duncan multiple range test.

Manurung *et al.* (2019; 3.62%). Differences in the wood diameter could cause a difference in yield. This research used *S. ligustrina* wood with a 14.5−17-cm diameter, whereas Manurung *et al.* (2019) used wood with a 7−10-cm diameter. The trees used in this study were older. The heartwood/sapwood ratio increases with increasing tree age, and the phytochemical content of heartwood from older trees is higher than that of younger trees (Arisandi *et al.,* 2024; Canal *et al.*, 2020).

The various woody stem parts of *S. ligustrina* influenced the phytochemical composition. According to the LC-MS/MS analysis, the chromatograms of heartwood, sapwood, and bark extracts were nearly identical, although the peak heights varied (Fig. 2). The identical chromatograms demonstrated that the phytochemical
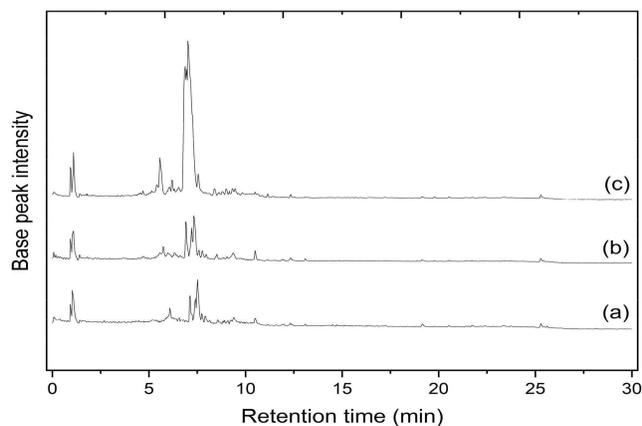
Fig. 2. Chromatograms of the sapwood (a), heartwood (b), and bark (c) extract of *Strychnos ligustrina*.

compounds in each extract were comparable, but their concentrations differed. This similarity could be observed at the retention time of 4–10 min. This range was considered a fingerprint area for the *S. ligustrina* wood extracts. Fig. 2 depicts the LCMS chromatograms, which consisted of 12 (heartwood), 13 (bark), and 10 peaks (sapwood). The most prominent spectral peaks, reflecting a molecular weight of 394.19 g/mol, were observed at retention times of 7.33 (heartwood), 7.14 (bark), and 7.53 min (sapwood).

Sixteen compounds with a database similarity index greater than 70% were identified in the heartwood, sapwood, and bark extracts (Table 2). Alkaloid compounds were abundant in the three extracts. Heartwood and sapwood extracts had a similar compound composition, containing three highly abundant nitrogen-containing compounds (strychnine, choline, and brucine), with strychnine being predominant (Table 2). The compound composition of bark extract was dramatically different from those of the heartwood and sapwood extracts, with the most abundant compounds being brucine and N-[1-(6,7-dimethoxy-1,2,3,4-tetrahydroisoquinoline-1-ylidene)-4-methyl-2-oxopentan-3-yl]benzamide. Syafii *et al.* (2016) reported that the alkaloids brucine and strychnine were present in the wood ethanol extract of *S. ligustrina*

and that they exhibit potent antimalarial activity. Brucine was also detected in other *Strychnos* species. Khasanah *et al.* (2024) described the presence of brucine in an *S. lucida* extract, and its content was correlated with antimalarial activity using an animal model. However, no other report detected N-[1-(6,7-dimethoxy-1,2,3,4-tetrahydroisoquinoline-1-ylidene)-4-methyl-2-oxopentan-3-yl]benzamide, which displayed high relative abundance in the bark of *S. ligustrina*.

3.2. *In vitro* antimalarial activity

The *in vitro* antimalarial assay demonstrates that all extracts could inhibit the growth of *P. falciparum* strain 3D7 (Fig. 3). Fig. 3(a–c) highlighted the concentration-dependent inhibitory effects of the extracts. However, the strength of the inhibitory effects of the bark, sapwood, and heartwood extracts varied by component. As presented in Fig. 3, 50% parasite growth inhibition was not achievable at extract concentrations of 0.01–10 μg/mL. Meanwhile, growth was restricted by more than 50% by concentrations of 50 and 100 μg/mL, with 100 μg/mL exhibiting the highest inhibition.

The antimalarial activity of aqueous extracts of various parts of *S. ligustrina* varied, with the IC_{50} ranging from

Table 2. The phytoconstituents of the aqueous extract of *Strychnos ligustrina* wood based on LC-MS/MS analysis

Compound	Retention time (min)	Molecular weight (g/mol)	Relative abundance (%)			Similarity index
			Sapwood	Bark	Heartwood	
Strychnine	7.706	335.16	15.187	0.063	16.261	93.5
Choline	1.237	104.09	13.889	2.841	15.094	95.5
Brucine	7.300	394.19	11.629	35.686	13.982	72.2
Proline	1.333	115.06	5.825	0.478	5.527	98.1
9-Ethyl-8-hydroxy-8,9,10,11,11a,12-hexahydro-6H-6,10:11,12a-dimethanoindolo[3,2-b]quinolizin-13-yl acetate	6.027	352.18	0.104	0.742	4.311	74.4
1,6-Dihydroxy-7-methyl-1,4a,5,6,7,7a-hexahydrocyclopenta[c]pyran-4-carboxylic acid methyl ester	7.171	228.10	0.018	0.006	2.33	75.3
N6-threonylcarbamoyladenosine	7.443	412.13	1.336	0.02	1.3	92.7
Pipecolinic acid	1.418	129.07	0.993	0.123	1.193	92.5
3,4-Bis(4-propan-2-ylanilino)cyclobut-3-ene-1,2-dione / BCD	7.345	348.18	1.246	4.233	1.169	90.4
(E)-methyl-2-((Z)-3-ethylidene-1,2,3,4,6,7,12,12b-octahydroindolo[2,3-a]quinolizin-2-yl)-3-hydroxy acrylate	6.322	352.18	0.038	5.153	0.926	80.6
2-[3-Ethenyl-5-(methoxycarbonyl)-2-{[(2S,3R,4S,5S,6R)-3,4,5-trihydroxy-6-(hydroxymethyl)oxan-2-yl]oxy}-3,4-dihydro-2H-pyran-4-yl]acetic acid	8.048	404.13	1.043	0.434	0.742	97.9
Koumine	5.984	306.17	0.895	7.243	0.525	94.2
(1S,3R,4S,5R)-3,5-bis({[(2E)-3-(3,4-dihydroxyphenyl)prop-2-enoyl]oxy})-1,4-dihydroxycyclohexane-1-carboxylic acid / DCA	10.000	516.12	0.51	0.097	0.463	97.1
6-formyl-2,3,3a1,4,5,6,11,12-octahydro-1H-3a,5a-ethanoindolizino[8,1-cd]carbazole-5-carboxylic acid	5.428	352.1	4.962	0.031	0.045	74.1
Quinine	7.568	324.18	0.004	2.783	0.002	93.8
N-[1-(6,7-dimethoxy-1,2,3,4-tetrahydroisoquinoline-1-ylidene)-4-methyl-2-oxopentan-3-yl]benzamide / NTB	10.836	408.21	0.000	22.331	0.001	76.1

10.14 to 17.30 μg/mL. Fig. 3(d) illustrates that the aqueous heartwood extract, with an IC_{50} of 10.14 μg/mL, had the strongest antimalarial activity, followed by the bark and sapwood extracts. The IC_{50} values of the sap-
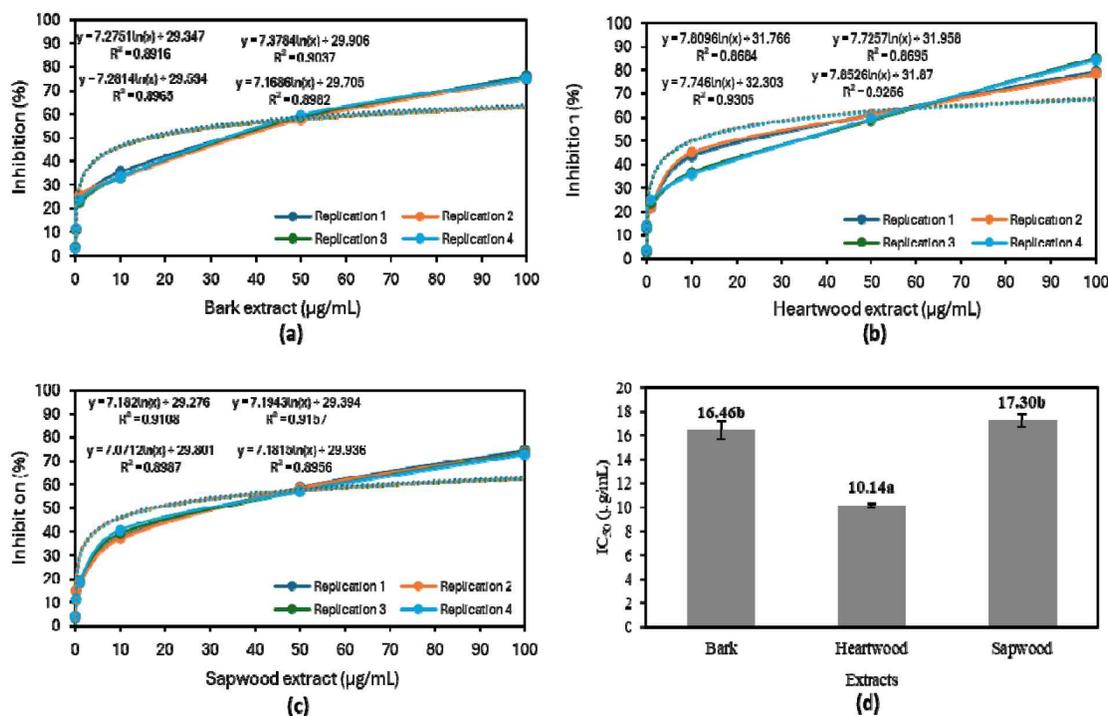
Fig. 3. The parasitemia inhibition of the bark (a), heartwood (b), sapwood (c) extracts and their IC_{50} value (d). [a,b] Numbers followed by different letters showed significantly different ($p < 0.05$) by Duncan's multiple range test. The dot-line in (a–c) described the trendline of logarithmic regression.

wood and bark extracts were not significantly different, although the value was slightly lower for the wood extract. This distinction is attributable to the nature and composition of the extractive components present in each extract (Miranda *et al.*, 2017). Alkaloids might be responsible for the extracts' effectiveness against malaria (Bekoe *et al.*, 2022; Belete *et al.*, 2020; Manurung *et al.*, 2019; Syafii *et al.*, 2016).

3.3. Molecular docking analysis

The phytoconstituents of *S. ligustrina* extracts exhibit low to high binding affinity for five proteins used from *P. falciparum.* The phytochemical compounds derived from the three extracts have varying binding affinity values towards the five target protein. Table 3 illustrates

that Brucine showed the best potential for lactate dehydrogenase, while DCA had the strongest interaction with M1 alanylaminopeptidase and plasmepsin II. Meanwhile, the PfNDH2 and falcilysin proteins showed the highest binding affinity with 3,4-bis(4-propan-2-ylanilino)cyclobut-3-ene-1,2 dione and strychnine, respectively. These compounds exhibited a higher binding affinity than chloroquine, a commonly used antimalarial drug (Tse *et al.*, 2019). To date, no studies have confirmed the *in vitro* mechanisms of these compounds binding to the five proteins used in this study. However, the potential of alkaloid compounds as antimalarials has been widely studied, yielding promising results (Uzor, 2020). These three compounds, which have different molecular structures, are classified as alkaloids. This structural difference results in varying binding affinities, which are also

Table 3. Binding affinity of *Strychnos ligustrina* phytochemical compounds

Phytochemical compound	Binding affinity (kcal/mol)				
	LD	M1-Ap	Plasmepsin II	PfNDH2	Falcilysin
Strychnine	−7.895 ± 0.013	−9.066 ± 0.009	−7.574 ± 0.006	−8.43 ± 0.006	−8.478 ± 0.004
2-[3-ethenyl-5-(methoxycarbonyl)-2-{[(2S,3R,4S,5S,6R)-3,4,5-trihydroxy-6-(hydroxymethyl)oxan-2-yl]oxy}-3,4-dihydro-2H-pyran-4-yl]acetic acid	−5.647 ± 0.008	−7.499 ± 0.009	−6.905 ± 0.008	−6.349 ± 0.014	−6.712 ± 0.467
3,4-Bis(4-propan-2-ylanilino)cyclobut-3-ene-1,2-dione / BCD	−7.869 ± 0.003	−9.191 ± 0.09	−8.407 ± 0.014	−10.198 ± 0.011	−7.788 ± 0.193
(1S,3R,4S,5R)-3,5-bis({[(2E)-3-(3,4-dihydroxyphenyl)prop-2-enoyl]oxy})-1,4-dihydroxycyclohexane-1-carboxylic acid / DCA	−7.143 ± 0.031	−9.940 ± 0.032	−8.766 ± 0.024	−8.704 ± 0.016	−8.274 ± 0.335
Choline	−3.302 ± 0.014	−3.703 ± 0.024	−3.349 ± 0.003	−3.502 ± 0.006	−3.383 ± 0.007
D-(+)-Pipecolinic acid	−5.63 ± 0.006	−5.615 ± 0.005	−5.005 ± 0.008	−6.196 ± 0.033	−4.939 ± 0.015
D-(+)-Proline	−5.439 ± 0.008	−5.087 ± 0.006	−4.457 ± 0.028	−5.46 ± 0.012	−4.529 ± 0.009
N6-threonylcarbamoyladenosine	−6.324 ± 0.031	−8.753 ± 0.021	−7.6 ± 0.002	−7.684 ± 0.009	−7.127 ± 0.046
Koumine	−6.786 ± 0.003	−7.904 ± 0.007	−8.114 ± 0.007	−8.829 ± 0.004	−7.966 ± 0.007
Quinine	−6.46 ± 0.024	−8.271 ± 0.07	−7.015 ± 0	−7.472 ± 0.016	−8.008 ± 0.006
Brucine	−7.94 ± 0.004	−9.427 ± 0.004	−8.089 ± 0.003	−8.044 ± 0.11	−7.905 ± 0.006
N-[1-(6,7-dimethoxy-1,2,3,4-tetrahydroisoquinolin-1-ylidene)-4-methyl-2-oxopentan-3-yl]benzamide / NTB	−6.868 ± 0.01	−8.541 ± 0.325	−8.399 ± 0.186	−9.584 ± 0.009	−7.631 ± 0.034
(E)-methyl 2-((Z)-3-ethylidene-1,2,3,4,6,7,12,12b-octahydroindolo[2,3-a]quinolizin-2-yl)-3-hydroxyacrylate	−6.907 ± 0.003	−8.441 ± 0.021	−7.629 ± 0.012	−9.326 ± 0.013	−8.091 ± 0.008
6-formyl-2,3,3a1,4,5,6,11,12-octahydro-1H-3a,5a-ethanoindolizino[8,1-cd]carbazole-5-carboxylic acid	−6.908 ± 0.006	−8.631 ± 0.005	−7.494 ± 0.023	−8.346 ± 0.006	−8.426 ± 0.005
9-ethyl-8-hydroxy-8,9,10,11,11a,12-hexahydro-6H-6,10:11,12a-dimethanoindolo[3,2-b]quinolizin-13-yl acetate	−6.918 ± 0.09	−8.153 ± 0.009	−7.214 ± 0.025	−8.076 ± 0.004	−7.747 ± 0.003
1,6-Dihydroxy-7-methyl-1,4a,5,6,7,7a-hexahydrocyclopenta[c]pyran-4-carboxylic acid methyl ester	−5.429 ± 0.002	−6.972 ± 0.04	−6.101 ± 0.002	−6.591 ± 0.007	−5.708 ± 0.007

related to their interactions with the target proteins.

An analysis of the interactions of the compounds with the best binding affinities with receptors revealed differences in the interactions formed by the best-docked

compounds compared to chloroquine as a positive control. In lactate dehydrogenase, brucine formed hydrogen bonds with Val[248] and Arg[171], while chloroquine did not form any hydrogen bonds [Fig. 4(a)]. A similar phenomenon was observed in falcilysin, where strychnine formed hydrogen bonds with Tyr[413], but no hydrogen
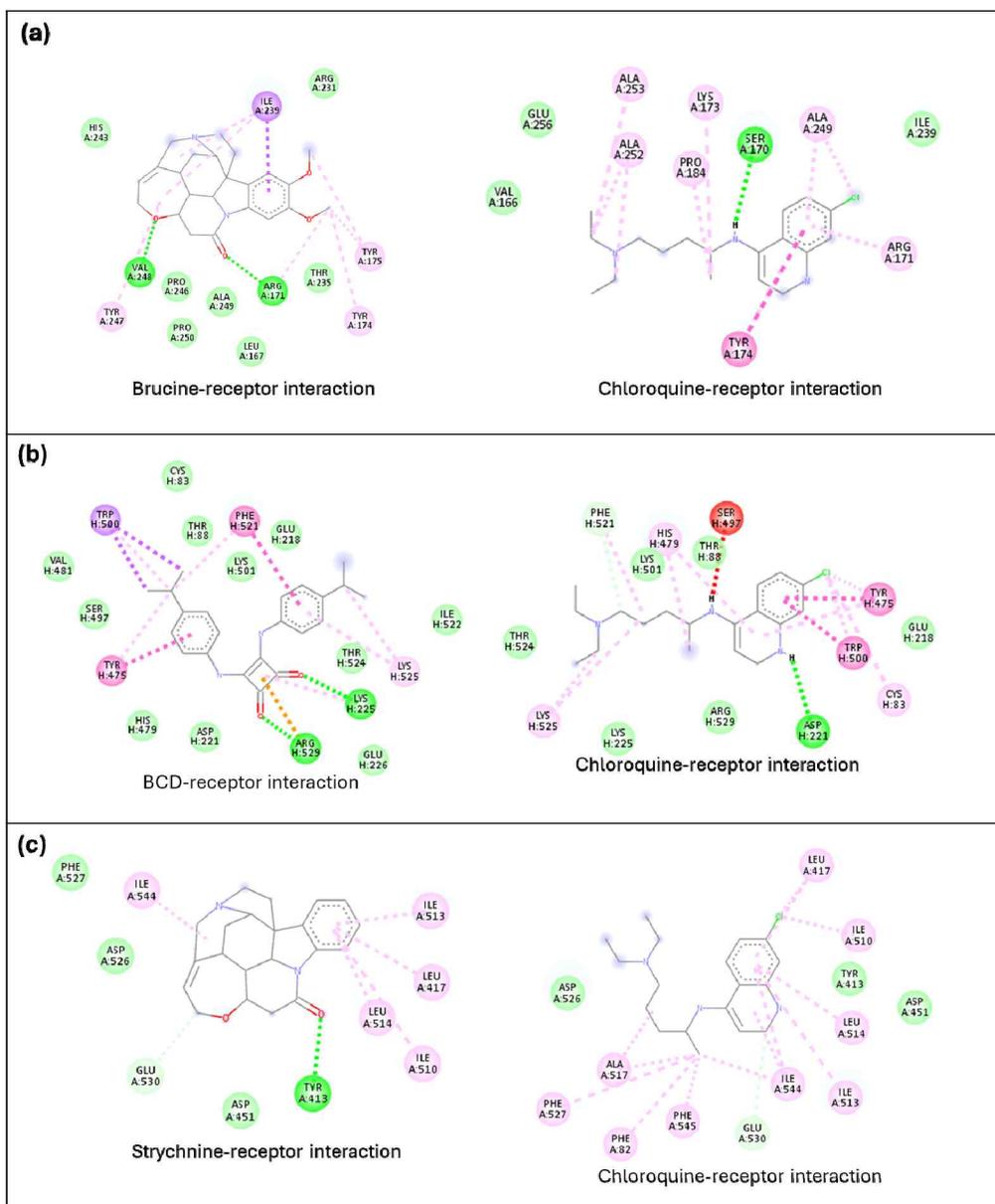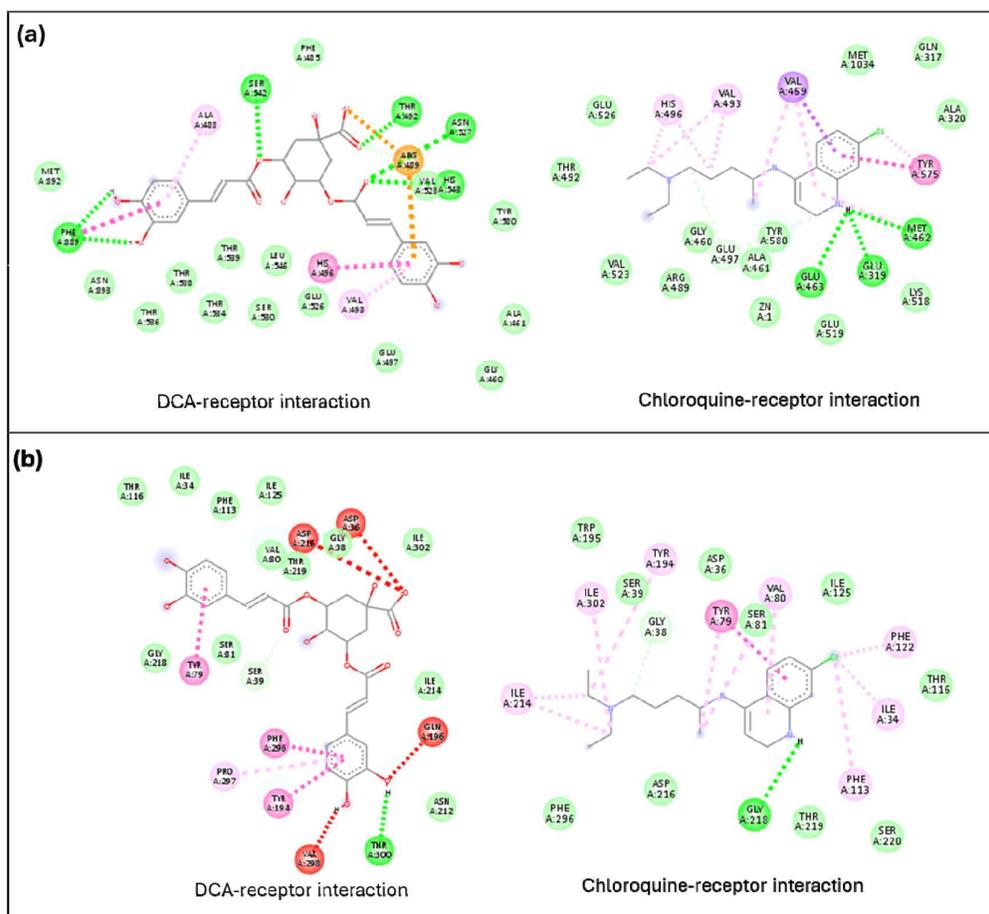

Fig. 4. The ligand-receptor interaction of the best docked ligands to lactate dehydrogenase (a), PfNDH2 (b), and falcilysin (c). BCD: 3,4-Bis(4-propan-2-ylanilino)cyclobut-3-ene-1,2-dione.

bonds were observed in the chloroquine-falcilysin interaction [Fig. 4(c)]. A different pattern was noted in the chloroquine-PfNDH2 interaction, where hydrogen bonds were present but fewer than in the BCD-PfNDH2 interaction [Fig. 4(b)]. As the active ingredient in antimalarial medications, chloroquine binds selectively to *P. falciparum* lactate dehydrogenase via NADH binding (Penna-Coutinho *et al.*, 2011). Wirjanata *et al.* (2024) also reported that chloroquine binds to and inhibits the function of falcilysin. However, this study

showed that many other phytochemical compounds have greater potency than chloroquine.

The DCA compound, which is the best-docked compound for M1 alanylaminopeptidase and plasmepsin II, showed differences in the interactions formed with each protein. The DCA interaction with M1 alanylaminopeptidase formed more hydrogen bonds [Fig. 5(a)]. Additionally, an important interaction in the DCA-M1 alanylaminopeptidase complex was the formation of a salt bridge. This interaction is believed to be a key

Fig. 5. The ligand-receptor interaction of the best docked ligands to M1 alanylaminopeptidase (a) and plasmepsin II (b). DCA: (1S,3R,4S,5R)-3,5-bis({[(2E)-3-(3,4-dihydroxyphenyl)prop-2-enoyl]oxy})-1,4-dihydroxycyclohexane -1-carboxylic acid.

factor in stabilizing the DCA-M1 alanylaminopeptidase complex. The stabilizing effect of salt bridges has also been confirmed through molecular dynamics studies on N-myristoyltransferase inhibitors, related to the treatment of protozoan infections (Spassov *et al.*, 2023). However, no studies have discussed the formation of salt bridges by DCA with M1 alanylaminopeptidase. The interaction with plasmepsin II protein showed a similar number of hydrogen bonds formed but with different amino acid residues. DCA formed more pi-pi interactions than chloroquine, which is believed to contribute to better complex formation.

The high strychnine content in heartwood is presumed to be the main factor contributing to the best antimalarial activity of heartwood extract. The heartwood extract contains more strychnine than the sapwood and bark extracts (Table 2). This compound also showed the highest binding affinity with falcilysin protein. Additionally, strychnine exhibited relatively high binding affinity with M1 alanylaminopeptidase and lactate dehydrogenase (Table 3). Based on this, the targeting of falcilysin protein is predicted to be the primary mechanism behind the antimalarial properties of heartwood extract. Philippe *et al.* (2006) reported the potent antiplasmodial activity of strychnine targeting the glycine receptor, which is highly correlated with the ether bond in the G-cycle of the strychnine molecular structure.

All the extracts studied in this research had IC$_{50}$ values below 20 μg/mL [Fig. 3(d)], indicating that they are all effective as antimalarials. Therefore, it is believed that these extracts may have specific mechanisms of action due to the distinct composition of compounds found in the sapwood and bark extracts. The sapwood has a compound profile similar to the heartwood, suggesting that its mechanism of action is likely similar to that of the heartwood extract (Table 2). In contrast, the bark extract has a composition significantly different from both the sapwood and heartwood. The bark contains high concentrations of brucine and BCD (Table 2),

which showed the best binding affinity to lactate dehydrogenase and PfNDH2, respectively (Table 3). The NTB compound also has a high abundance in the bark extract (Table 2), and this compound has a fairly high binding affinity for plasmepsin and PfNDH2 proteins (Table 3). This suggests that the antimalarial activity of the bark extract is related to the inhibition of several proteins. Additionally, the compound DCA, identified as the best-docked compound in M1 alanylaminopeptidase [Fig. 5(a)], was present at low concentrations in all three extracts, indicating that it may also contribute to the antimalarial activity across the extracts.

Although some compounds may have stronger or weaker activities, each compound contributes to antimalarial activity because the study used an extract containing various of compounds. Study Na and Kim (2022) and Yoon and Kim (2023) proved that a combination of extracts with a greater variety of compounds than a single extract had higher antifungal activity than a single extract. Some compounds have been shown to work synergistically as antifungals. However, there is a tendency for certain proteins to have a more significant effect than other proteins. It is confirmed through the heartwood extract, which has the highest levels of strychnine (Table 2) and the highest binding affinity to falcylisin (Table 3). It is believed to enhance its antimalarial effects. In addition, the high content of brucine in the bark also had a good effect on the antimalarial activity of the bark extract (IC$_{50}$ < 20 μg/mL). However, the effect was not as good as that of strychnine observed in the heartwood extract.

4. CONCLUSIONS

The extractive yields of *S. ligustrina* using a water-based solvent differed among the various parts of the wood, with the highest yield obtained from the heartwood extract. In terms of effectiveness, the heartwood extract demonstrated a stronger inhibition of *P.*

falciparum compared to the sapwood and bark extracts. However, the IC_{50} values of all *S. ligustrina* extracts from different parts of the stem were below 20 μg/mL, confirming their potency as antimalarial agents. LC-MS/MS analysis indicated that, although the extracts shared a similar chemical composition, the concentrations of individual components varied. Strychnine was the dominant compound in both the heartwood and sapwood, while brucine was more prevalent in the bark. Strychnine, which is the most abundant compound in the heartwood, exhibited the strongest potential for binding to the falcilysin protein. Additionally, other compounds with strong molecular binding activity suggest potential for further exploration of these specific protein interactions.

CONFLICT of INTEREST

No potential conflict of interest relevant to this article was reported.

ACKNOWLEDGMENT

REFERENCES

Andianto, Wahyudi, I., Sari, R.K., Pari, G., Prayogo, Y.H. 2024. Phytochemical profile of *Rhizophora apiculata, Bgruguiera gymnorhiza*, and *Bruguiera cylindrica* for wood identification. Jurnal Sylva Lestari 12(2): 435-444.

Arinana, A., Dharma, R.A., Sari, R.K., Rahmawati, A.I., Andika, R., Nandika, D. 2024. Bioactivity of cajuput seedling *n*-hexane extract as an attractant for subterranean termite *Coptotermes curvignathus* Holmgren (Isoptera: Rhinotermitidae). Journal of the Korean Wood Science and Technology 52(1): 31-46.

Arisandi, R., Takahashi, K., Nirsatmanto, A., Sunarti, S., Rimbawanto, A., Putri, A.I., Kartikawati, N.K., Haryjanto, L., Herawan, T., Lestari, F., Lukmandaru, G. 2024. Analysis of lipophilic constituents related to heartwood formation in young *Swietenia mahagoni* (L.) Jacq trees. Journal of the Korean Wood Science and Technology 52(1): 13-30.

Aulia, M.I., Sari, R.K., Nawawi, D.S., Dewi, R.T. 2022. Isolation and identification of antioxidant and α-glucosidase inhibitor compound from prospective extract of acacia bark from Indonesia. Research Journal of Pharmacy and Technology 15(9): 3847-3853.

Bekoe, S.O., Orman, E., Adjabui, S.A., Brobbey, A.A., Oppong-Kyekyeku, J., Opuni, K.F.M. 2022. Development and validation of an ion-pair HPLC-UV method for the quantitation of quinoline and indoloquinoline alkaloids in herbal and pharmaceutical antimalarial formulations. Journal of Chemistry 2022: 4625954.

Belete, T.M. 2020. Recent progress in the development of new antimalarial drugs with novel targets. Drug Design, Development and Therapy 14: 3875-3889.

Cahyaningsih, U., Sa'diah, S., Syafii, W., Sari, R.K., Maring, A.J., Nugraha, A.B. 2022. Antimalarial efficacy of aqueous extract of *Strychnos ligustrina* and its combination with dihydroartemisinin and piperaquine phosphate (DHP) against *Plasmodium berghei* infection. Korean Journal of Parasitology 60(5): 339-344.

Cahyaningsih, U., Sa'diah, S., Syafii, W., Sari, R.K., Maring, A.J., Nugraha, A.B. 2023. Comparison of the combinations of water and ethanol extract of *Strychnos ligustrina* blum wood with dihydroartemisinin-piperaquin phosphate (DHP) as an anti-

malaria in mice infected *P. berghei* ANKA. IOP Conference Series: Earth and Environmental Science 1174(1): 012015.

Canal, W.D., Macedo Ladeira Carvalho, A.M., Oliveira Carneiro, A.C., Vidaurre, G.B., de Freitas, F.P., de Magalhes, M.A. 2020. Effect of age on heartwood / sapwood relationship, extractive content, and permeability of teak wood. Floresta 50(4): 1698-1706.

Dunn, C.R., Banfield, M.J., Barker, J.J., Higham, C.W., Moreton, K.M., Turgut-Balik, D., Brady, R.L., Holbrook, J.J. 1996. The structure of lactate dehydrogenase from *Plasmodium falciparum* reveals a new target for anti-malarial design. Nature Structural Biology 3(11): 912-915.

Ella Nkogo, L.F., Bopenga Bopenga, C.S.A., Ngohang, F.E., Mengome, L.E., Aboughe Angone, S., Edou Engonga, P. 2022. Phytochemical and anti-termite efficiency study of *Guibourtia tessmanii* (*harms*) J. Léonard (Kévazingo) bark extracts from Gabon. Journal of the Korean Wood Science and Technology 50(2): 113-125.

Familasari, S., Sari, R.K., Syafii, W., Carolina, A., Cahyaningsih, U., Sa'diah, S. 2023. Ultrasound-assisted extraction of antimalarial compounds from the bidara laut (*Strychnos ligustrina*) heartwood. Jurnal Sylva Lestari 11(3): 360-369.

Giacometti, M., Milesi, F., Coppadoro, P.L., Rizzo, A., Fagiani, F., Rinaldi, C., Cantoni, M., Petti, D., Albisetti, E., Sampietro, M., Ciardo, M., Siciliano, G., Alano, P., Lemen, B., Bombe, J., Nwaha Toukam, M.T., Fernand Tina, P., Rita Gismondo, M., Corbellino, M., Grande, R., Beniamino Fiore, G., Ferrari, G., Antinori, S., Bertacco, R. 2021. A lab-on-chip tool for rapid, quantitative, and stage-selective diagnosis of malaria. Advanced Science 8(14): 2004101.

Huynh, Q.H. 2016. Efficacy of dihydroartemisinin-piperaquine and chloroquine in treating uncomplicated *Plasmodium falciparum* and *Plasmodium vivax* malaria in Vietnam. American Journal of Tropical Medicine and Hygiene 95(5): 478-479.

Indonesian Ministry of Health. 2023. Indonesia Health Profile 2022. Indonesian Ministry of Health, Jakarta, Indonesia.

Khasanah, U., Nurrahmah, Q.I., Amalia, T., Putri, Z.N., Mufidah, I., Napik, R., Lyrawati, D., Ihsan, B.R.P., Febrianti, M.E. 2024. Oral acute toxicity study and *in vivo* antimalarial activity of *Strychnos lucida* R. Br. tablet. Journal of Ethnopharmacology 330: 118200.

Lin, J., Yan, X., Chung, Z., Liew, C.W., El Sahili, A., Pechnikova, E.V., Preiser, P.R., Bozdech, Z., Gao, Y.G., Lescar, J. 2024. Inhibition of falcilysin from *Plasmodium falciparum* by interference with its closed-to-open dynamic transition. Communications Biology 7(1): 1070.

Manurung, H., Sari, R.K., Syafii, W., Cahyaningsih, U., Ekasari, W. 2019. Antimalarial activity and phytochemical profile of ethanolic and aqueous extracts of bidara laut (*Strychnos ligustrina* Blum) wood. Journal of the Korean Wood Science and Technology 47(5): 587-596.

Miranda, I., Sousa, V., Ferreira, J., Pereira, H. 2017. Chemical characterization and extractives composition of heartwood and sapwood from *Quercus faginea*. PLOS ONE 12(6): e0179268.

McGowan, S., Porter, C.J., Lowther, J., Stack, C.M., Golding, S.J., Skinner-Adams, T.S., Trenholme, K.R., Teuscher, F., Donnelly, S.M., Grembecka, J., Mucha, A., Kafarski, P., DeGori, R., Buckle, A.M., Gardiner, D.L., Whisstock, J.C., Dalton, J.P. 2009. Structural basis for the inhibition of the essential *Plasmodium falciparum* M1 neutral aminopeptidase. Proceedings of the National Academy of Sciences 106(8): 2537-2542.

Mishra, V., Rathore, I., Arekar, A., Sthanam, L.K., Xiao, H., Kiso, Y., Sen, S., Patankar, S., Gustchina, A., Hidaka, K., Wlodawer, A., Yada, R.Y., Bhaumik, P.

2018. Deciphering the mechanism of potent peptidomimetic inhibitors targeting plasmepsins: Biochemical and structural insights. The FEBS Journal 285(16): 3077-3096.

Morais, M.C., Pereira, H. 2012. Variation of extractives content in heartwood and sapwood of *Eucalyptus globulus* trees. Wood Science and Technology 46(4): 709-719.

Na, H., Kim, T.J. 2022. Synergistic antifungal activity of Phellodendri Cortex and Magnoliae Cortex against *Candida albicans*. Journal of the Korean Wood Science and Technology 50(1): 12-30.

Orozco, M.I., Moreno, P., Guevara, M., Abonia, R., Quiroga, J., Insuasty, B., Barreto, M., Burbano, M.E., Crespo-Ortiz, M.P. 2024. *In silico* prediction and *in vitro* assessment of novel heterocyclics with antimalarial activity. Parasitology Research 123(1): 75.

Penna-Coutinho, J., Cortopassi, W.A., Oliveira, A.A., França, T.C.C., Krettli, A.U. 2011. Antimalarial activity of potential inhibitors of *Plasmodium falciparum* lactate dehydrogenase enzyme selected by docking studies. PLOS ONE 6(7): e21237.

Philippe, G., Angenot, L., De Mol, P., Goffin, E., Hayette, M.P., Tits, M., Frédérich, M. 2005. *In vitro* screening of some *Strychnos* species for antiplasmodial activity. Journal of Ethnopharmacology 97(3): 535-539.

Philippe, G., Nguyen, L., Angenot, L., Frédérich, M., Moonen, G., Tits, M., Rigo, J.M. 2006. Study of the interaction of antiplasmodial strychnine derivatives with the glycine receptor. European Journal of Pharmacology 530(1−2): 15-22.

Prayogo, Y.H., Batubara, I., Wahyudi, S.T., Sari, R.K., Syafii, W. 2023. Metabolite profile, antiproliferative, and antioxidant activity of *Acacia auriculiformis* and *Acacia crassicarpa* extracts. Journal of Saudi Chemical Society 27(6): 101742.

Sadiah, S., Syafii, W., Sari, R.K., Sani, Y., Alfarisi, H., Andini, H.F., Nuraliyu, R.I., Cahyaningsih, U. 2023. Subchronic toxicity test of *Strychnos ligustrina* extract and dihydroartemisinin-piperaquine phosphate in male and female mice. Journal of Applied Pharmaceutical Science 13(4): 220-230.

Setiawan, O., Wahyuni, N., Susila, W.W., Rahayu, A.A.D., Rostiwati, T. 2014. Bidara laut (*Strychnos ligustrina* Blume) syn. *S. lucida* R. Br Sumber Bahan Obat Potensial di Nusa Tenggara Barat dan Bali. FORDA, Bogor, Indonesia.

Spassov, D.S., Atanasova, M., Doytchinova, I. 2023. A role of salt bridges in mediating drug potency: A lesson from the *N*-myristoyltransferase inhibitors. Front Mol Biosci 9: 1066029.

Syafii, W., Sari, R.K., Cahyaningsih, U., Anisah, L.N. 2016. Antimalarial activity of the fractions from ethanol extract of *Strychnos ligustrina* blume. wood. Research Journal of Medicinal Plants 10(6-7): 403-408.

Taek, M.M. 2023. Kayu Ular: Etnomedisin, Fitokimia, aktivitas dan Toksisitas obat Tradisional Antimalaria Andalan orang Timor. Rena Cipta Mandiri, Malang, Indonesia.

Tse, E.G., Korsik, M., Todd, M.H. 2019. The past, present and future of anti-malarial medicines. Malaria Journal 18(1): 93.

Uzor, P.F. 2020. Alkaloids from plants with antimalarial activity: A review of recent studies. Evidence-Based Complementary and Alternative Medicine 2020: 8749083.

World Health Organization. 2023. World malaria report 2023. https://www.who.int/teams/global-malaria-programme/reports/world-malaria-report-2023

Wirjanata, G., Lin, J., Dziekan, J.M., El Sahili, A., Chung, Z., Tjia, S., Zulkifli, N.E.B., Boentoro, J., Tham, R., Jia, L.S., Go, K.D., Yu, H., Partridge, A., Olsen, D., Prabhu, N., Sobota, R.M., Nordlund, P., Lescar, J., Bozdech, Z. 2024. Identification of an inhibitory pocket in falcilysin provides a new

avenue for malaria drug development. Cell Chemical Biology 31(4): 743-759.E8.

Yang, Y., Yu, Y., Li, X., Li, J., Wu, Y., Yu, J., Ge, J., Huang, Z., Jiang, L., Rao, Y., Yang, M. 2017. Target elucidation by cocrystal structures of NADH-ubiquinone oxidoreductase of *Plasmodium falciparum* (*Pf*NDH2) with small molecule to eliminate drug-resistant malaria. Journal of Medicinal Chemistry 60(5): 1994-2005.

Yoon, J., Kim, T.J. 2023. Synergistic growth inhibition of herbal plant extract combinations against *Candida albicans*. Journal of the Korean Wood Science and Technology 51(2): 145-156.

Zalsabila, A., Syafii, W., Priadi, T., Syahidah. 2024. Anti-termite activity of tamanu bark extract (*Calophyllum inophyllum* L.). Journal of the Korean Wood Science and Technology 52(2): 134-144.